Hindawi
Wireless Communications and Mobile Computing
Volume 2019, Article ID 6097686, 11 pages
https://doi.org/10.1155/2019/6097686

*Research Article*

# Performance Analysis of Energy Harvesting-Based Full-Duplex Decode-and-Forward Vehicle-to-Vehicle Relay Networks with Nonorthogonal Multiple Access

**Ba Cao Nguyen,[1] Tran Manh Hoang,[1] Xuan Nghia Pham,[1] and Phuong T. Tran [2]**

[1]*Faculty of Radio Electronics, Le Quy Don Technical University, Hanoi, Vietnam*
[2]*Wireless Communications Research Group, Faculty of Electrical and Electronics Engineering, Ton Duc Thang University, Ho Chi Minh City, Vietnam*

Correspondence should be addressed to Phuong T. Tran; tranthanhphuong@tdtu.edu.vn

Received 3 July 2019; Revised 24 September 2019; Accepted 15 October 2019; Published 3 November 2019

Academic Editor: Miguel López-Benítez



In this paper, a combination of energy harvesting (EH) and cooperative nonorthogonal multiple access (NOMA) has been proposed for full-duplex (FD) relaying vehicle-to-vehicle (V2V) networks with two destination nodes over a Rayleigh fading channel. Different from previous studies, here both source and relay nodes are supplied with the energy from a power beacon (PB) via RF signals, and then use the harvested energy for transmitting the information. For the extensive performance analysis, the closed-form expressions for the performance indicators, including outage probability (OP) and ergodic capacity of both users, have been derived rigorously. Additionally, the effect of various parameters, such as EH time duration, residual self-interference (RSI) level, and power allocation coefficients, on the system performance has also been investigated. Furthermore, all mathematical analytical results are confirmed by Monte-Carlo simulations, which also demonstrate the optimal value of EH time duration to minimize the OP and maximize the ergodic capacity of the proposed system.

## 1. Introduction

Under the fast development of Internet of Things (IoT) devices and future wireless networks, e.g., the fifth generation (5G) of mobile communications and numerous solutions to improve the spectrum efficiency have been proposed and experimented. Among those solutions, the advanced techniques such as full-duplex (FD) relaying, nonorthogonal multiple access (NOMA), and massive multiple-input multiple-output (MIMO) have been arising as the most promising candidates [1–3]. Therefore, a lot of studies and experiments have been conducted to investigate those systems in practical scenarios to verify the potential of capacity increasing. Due to the fact that the FD communication can achieve double of system capacity compared to half-duplex (HD) with perfect self-interference (SI) cancellation, the study of FD systems becomes a hot topic. On the contrary, NOMA can improve the average system capacity in comparison with the traditional orthogonal multiple access (OMA) because it can help exchange information among multiple users at the same time, in the same frequency band, only with different power allocation coefficients.

The combination between FD communication and NOMA technique has been studied in the literature such as [4–7]. In [4], the authors analyzed the down-link NOMA system with a FD amplify-and-forward (AF) relay. In that work, the direct link from the source node to near user has been considered. Through numerical calculation, the authors obtained the analytical expressions to indicate the system performance, including outage probabilities (OPs) and ergodic capacities of both users. Based on that, the impact of residual self-interference (RSI) and power allocation coefficients were also investigated. In another aspect, Yue et al. [6] have utilized a cooperative NOMA system where the near user was employed as a relay, which can operate in either HD or FD mode and with decode-and-forward (DF) protocol. The authors considered two cases,

i.e., with or without a direct link from the base station (BS) to the far user. OP expressions, ergodic rate, and energy efficiency have been derived for system performance analysis. Similar to [6], Zhang et al. [7] also considered a NOMA system, in which the near user operated as a FD relay to forward the signal to the far user. The authors derived the OP expressions of both users and compared with the conventional NOMA and OMA schemes.

Recently, various techniques have been applied for energy supply for wireless networks, including RF energy harvesting (EH) [5, 8–11]. Specifically, wireless devices first harvest energy from radio frequency signals and then use the harvested energy for exchanging data. Therefore, the EH technique is a promising solution for battery-limited devices. Due to the advantage of wireless charging, EH becomes popular in real-world applications such as personal mobile phones. Furthermore, to increase the amount of harvested energy at the transmitters, power beacon (PB) may be utilized to supply energy wirelessly to both source and relay before information transmission [10, 12–14].

In the literature, there have been several studies on the combination of EH, FD, and NOMA [5, 9, 15–17]. In [9], the authors considered a down-link NOMA system, where the source node transmits two signals to two users via a FD decode-and-forward relay node. In this model, the relay node has constrained power supply and must harvest energy through RF signals transmitted by the source. Based on the theoretical analysis, the authors derived OP of the considered system over Nakagami-$m$ fading channel. Additionally, the optimal harvesting time and optimal power allocation coefficients to minimize OP were also obtained. In 2018, Alsaba et al. [5] investigated a cooperative NOMA system, where a strong user operated at the FD mode and forwarded the signal to a weak user. The authors successfully derived OP expressions for both users and studied the impact of imperfect self-interference and EH circuit on the system performance. Wang and Wu [15] and Guo et al. [16] investigated a similar system where the strong user (which is an EH-FD relay node) harvested energy from the source node for transmitting information messages. Furthermore, [17] extended this model to $M$ relay nodes and $K$ users. Different from [5, 9, 15, 16], the work in [17] investigated the case that the users harvest energy from the source. In summary, the previous studies considered either only FD relay (strong user) or weak user can harvest energy from the source. The case that both source and relay harvest energy from the power beacon has not been investigated.

Although the EH, FD, and NOMA are advanced techniques that play a key role for future wireless networks, the coexistence of these techniques in a unique system raises the complexity of processing to a very high level. However, with the fast development of circuit design as well as analog and digital processing techniques, hopefully the proposed system can be implemented in very near future. On the contrary, in practical networks, not only the relay node but also the source node has limited power supply. That leads to the idea of providing the energy to the source node before message transmission by using the power beacon (PB). With tremendous number of applications in many areas [18], FD communication has been considered particularly for vehicle-to-vehicle (V2V) communication networks. When vehicles move on the road, the end-to-end delay of the information transmission among them can be reduced significantly by applying FD communication. Moreover, with the ability to send and receive data simultaneously, the innovative technologies, such as cooperative, semi-autonomous, and autonomous driving, can be supported. As a result, road and passenger safety is enhanced and traffic congestion is reduced. Because of the mobility of vehicles, it is difficult to supply energy to the wireless devices on the vehicle. To maintain the connectivity to other devices, they need to harvest energy from the RF signals for powering the data transmission. Therefore, EH is a promising solution for V2V networks.

Motivated by all these above facts, in this paper, we investigate an EH-FD-NOMA system, in which both source and relay nodes harvest energy from PB. After that, they utilize suitable circuits to transform the harvested energy to power for transmitting information. Furthermore, the relay node operates in the FD mode while the source node and two users operate in the half-duplex (HD) mode. Two users are located in different location from the relay. In particular, there is a strong user and the other is a weak user. Based on the analytical expressions of outage probability and ergodic capacities at both users, we investigate the system performance of the proposed system. The contributions of this paper can be summarized as follows:

(i) We proposed a novel combination of EH, FD, and NOMA techniques in V2V networks. It is noted that in the previous studies about the similar combination, only the case that a strong user acts as a relay has been considered. In addition, only the relay can harvest the energy from the source node. In our model, we assume that both the source node and the FD relay node, which is not any one of the receiving users, harvest the energy from the power beacon through RF signals. This assumption leads to the complexity in mathematical derivations of the proposed system performance, compared with previous works. However, our model can be applied for V2V communication systems and future wireless networks, thus it is vital to investigate.

(ii) We derive the exact theoretical expressions for the system performance in terms of outage probability, throughput, and ergodic capacity of both users in the case of imperfect self-interference cancellation at the FD relay node over Rayleigh fading channel.

(iii) We analyze the system performance through analysis and simulation. The numerical results show that, with the suitable power allocation coefficients for both users, the performance measures of both users are the same. On the contrary, the impact of imperfect self-interference cancellation and the time for harvesting are also analyzed. In fact, there exists

an optimal time duration for EH to minimize outage probability and maximize ergodic capacity. Finally, we conduct Monte-Carlo simulations to validate the analytical results.

The rest of this paper is organized as follows: Section 2 presents the system model, while Section 3 derives the system performance in terms of OP and capacity. Section 4 discusses about the numerical results and finally, Section 5 concludes this paper.

## 2. System Model

In this section, we introduce a system model that combines three techniques EH, FD, and NOMA, as illustrated in Figure 1. Here, the source node (S) simultaneously transmits two messages to both users ($D_1$ and $D_2$) under the assistance of relay node (R). We assume that S and R do not have their all power supplies due to their inconvenient locations. As a result, they must harvest the energy from RF signals. To supply enough power for S and R, we use a power beacon (PB) to transmit energy to them. After the energy harvesting phase, S and R convert the received energy to the power for transmitting signals. As shown in Figure 1, PB, S, $D_1$, and $D_2$ are single-antenna devices while R is equipped with two antennas. In this system, only R operates at the FD mode, while other devices operate in the HD mode. In many analytical studies and experiments, R can use one shared-antenna for transmitting/receiving the signal. However, in this work, we deploy two-antenna relay to identify clearly the SI and get the better SI cancellation. To transmit simultaneously two messages to two users, S applies the NOMA technique in the power domain. Assume that the distances from two users to R are different. In particular, $D_1$ is a far user and $D_2$ is a near user.

The operation of the EH-FD-NOMA system of interest is divided into two stages. During the first stage, PB transmits a RF signal to S and R. S and R harvest the energy through this RF signal and then convert it to the supply power. During the second stage, by using the harvested energy, S transmits a message to R, and at the same time R transmits the decoded message from the previous block to $D_1$ and $D_2$. Let $T$ be the length of the entire transmission block. The time duration for the first stage is $\alpha T$, while the time duration for the second stage is $(1-\alpha)T$, where $\alpha$ is called time-switching ratio, $0 \le \alpha \le 1$. Figure 2 illustrates the time duration for EH and for information transmission.

Let $E_h^S$ and $E_h^R$ denote the harvested energies at S and R during the EH phase $\alpha T$. Therefore, $E_h^S$ and $E_h^R$ are given as [19].

$$E_h^S = \eta \alpha T P |h_{BS}|^2, \quad E_h^R = \eta \alpha T P |h_{BR}|^2, \tag{1}$$

where $\eta$ is a constant that represents the energy conversion efficiency. Its value depends on the converting hardware and method $(0 \le \eta \le 1)$; $P$ is the average transmit power of PB; and $h_{BS}$ and $h_{BR}$ are, respectively, the fading coefficients of the channels from PB to S and from PB to R. As illustrated in

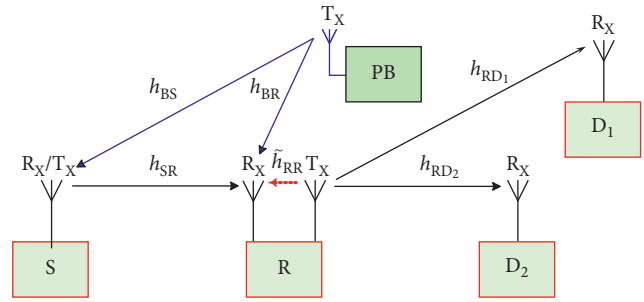


Figure 1: System model of the proposed EH-FD-NOMA system.

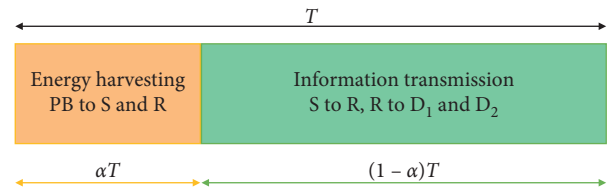


Figure 2: Data frame structure of the time duration for EH and information.

Figure 1, in this paper, we investigate the case that R only uses one antenna for EH. In practical systems, R can use all antennas for harvesting energy by using suitable hardware resources [20]. Furthermore, S and R have a super capacitor to store the harvested energy. After the time duration $\alpha T$ of EH, S and R can fully use the harvested energy for transmitting information during the time $(1-\alpha)T$. Therefore, the transmit power at S and R can be calculated as [21].

$$P_S = \frac{\eta \alpha P |h_{BS}|^2}{1-\alpha} = \frac{\eta \alpha P \rho_1}{1-\alpha}, \quad P_R = \frac{\eta \alpha P |h_{BR}|^2}{1-\alpha} = \frac{\eta \alpha P \rho_2}{1-\alpha}, \tag{2}$$

where $\rho_1 = |h_{BS}|^2$ and $\rho_2 = |h_{BR}|^2$ are channel gains of the links PB $\longrightarrow$ S and PB $\longrightarrow$ R, respectively.

During the time duration $(1-\alpha)T$, S transmits a signal to R. Simultaneously, R forwards a signal to both users $D_1$ and $D_2$ on the same frequency band. That results in SI at R. It is also noted that the message that is transmitted by S are the combination of two messages for two users $D_1$ and $D_2$. The messages transmitted by R are the decoded messages at R during the previous symbol block (as long as R decodes successfully the received message). The received signal at R can be calculated as

$$y_R = h_{SR}\left(\sqrt{a_1 P_S}\, x_1 + \sqrt{a_2 P_S}\, x_2\right) + \tilde{h}_{RR}\sqrt{P_R} x_R + z_R, \tag{3}$$

where $h_{SR}$ and $\tilde{h}_{RR}$ are, respectively, the fading coefficients of the channels from S $\longrightarrow$ R and from the transmitting to the receiving circuits of R; $a_1$ and $a_2$ are NOMA coefficients with $a_1 > a_2$; $P_S$ and $P_R$ are average transmit powers at S and R, respectively; $x_1$ and $x_2$ are two messages for two users $D_1$ and $D_2$, respectively; $x_R$ is the transmitted signals at R; and $z_R$ is the additive white Gaussian noise (AWGN) with zero-mean and variance of $\sigma^2$, i.e., $z_R \sim C\mathcal{N}(0, \sigma^2)$.

From (3), the SI at R is calculated by

$$\mathbb{E}\left\{\left|\widetilde{h}_{\mathrm{RR}}\right|^2 P_{\mathrm{R}}\right\} = \frac{\eta\alpha P}{1-\alpha}\mathbb{E}\left\{\left|\widetilde{h}_{\mathrm{RR}}\right|^2 \rho_2\right\}. \tag{4}$$

In FD devices, various SI cancellation techniques can be applied to reduce the effect of RSI on the system performance such as isolation, propagation domain, and digital and analog cancellation. In fact, the relay definitely knows the transmit signal $x_{\mathrm{R}}$, so by using the results of SI channel estimation of $\widetilde{h}_{\mathrm{RR}}$, it can apply digital processing methods to subtract the SI from the received signals [22–25]. However, due to the hardware impairment and the imperfect estimation of the SI channel, SI may still exist in the system after applying various SI cancellation methods and degrade the system performance. Typically, the RSI, which is denoted by $I_{\mathrm{R}}$, can be modeled by the complex Gaussian distribution [23, 25–28] with zero-mean and variance $\gamma_{\mathrm{RSI}}$, where $\gamma_{\mathrm{RSI}} = \widetilde{\Omega}(\eta\alpha P)/(1-\alpha)$. It is also noted that $\widetilde{\Omega}$ denotes the SI cancellation capability of the relay node. After SI cancellation, (3) becomes

$$y_{\mathrm{R}} = h_{\mathrm{SR}}\left(\sqrt{a_1 P_{\mathrm{S}}}\, x_1 + \sqrt{a_2 P_{\mathrm{S}}}\, x_2\right) + I_{\mathrm{R}} + z_{\mathrm{R}}. \tag{5}$$

From (5), SINR (signal-to-interference-plus-noise ratio) to detect the message $x_1$ at R (denoted by $\gamma_{\mathrm{R}}^{x_1}$) is calculated as

$$\gamma_{\mathrm{R}}^{x_1} = \frac{\left|h_{\mathrm{SR}}\right|^2 a_1 P_{\mathrm{S}}}{\left|h_{\mathrm{SR}}\right|^2 a_2 P_{\mathrm{S}} + \gamma_{\mathrm{RSI}} + \sigma^2} = \frac{a_1\eta\alpha P\rho_1\rho_3}{a_2\eta\alpha P\rho_1\rho_3 + (\gamma_{\mathrm{RSI}} + \sigma^2)(1-\alpha)}, \tag{6}$$

where $\rho_3 = |h_{\mathrm{SR}}|^2$ is the channel gain from S $\longrightarrow$ R.

After detecting $x_1$, R removes all $x_1$'s components from received signals and then detect $x_2$. Thus, SINR to detect message $x_2$ at R (denoted by $\gamma_{\mathrm{R}}^{x_2}$) is given by

$$\gamma_{\mathrm{R}}^{x_2} = \frac{a_2\eta\alpha P\rho_1\rho_3}{(\gamma_{\mathrm{RSI}} + \sigma^2)(1-\alpha)}. \tag{7}$$

Due to the FD mode, during the time duration of $(1-\alpha)T$, R transmits the signals to both destinations $\mathrm{D}_1$ and $\mathrm{D}_2$. We assume that the delay caused by signal processing at the relay is equal to one symbol period. Therefore, the transmitted signals at R are the received signals in the previous period after processing. Then, the received signals at $\mathrm{D}_1$ and $\mathrm{D}_2$ are, respectively, given by

$$y_{\mathrm{D}_1} = h_{\mathrm{RD}_1}\left(\sqrt{a_1 P_{\mathrm{R}}}\, x_1 + \sqrt{a_2 P_{\mathrm{R}}}\, x_2\right) + z_1, \tag{8}$$

$$y_{\mathrm{D}_2} = h_{\mathrm{RD}_2}\left(\sqrt{a_1 P_{\mathrm{R}}}\, x_1 + \sqrt{a_2 P_{\mathrm{R}}}\, x_2\right) + z_2, \tag{9}$$

where $h_{\mathrm{RD}_1}$ and $h_{\mathrm{RD}_2}$ are fading coefficients of channels from R $\longrightarrow$ $\mathrm{D}_1$ and R $\longrightarrow$ $\mathrm{D}_1$, respectively and $z_1$ and $z_2$ are the AWGN terms with zero-mean and variance of $\sigma^2$, i.e., $z_1 \sim C\mathcal{N}(0,\sigma^2)$ and $z_2 \sim C\mathcal{N}(0,\sigma^2)$.

By the principle of NOMA systems, the far user (user 1, denoted by $\mathrm{D}_1$ in our paper) decodes its own message while user 2's message is considered as interference. The near user (user 2 or $\mathrm{D}_2$ in this paper) first subtracts the signal of the user $\mathrm{D}_1$ through successive interference cancellation (SIC) to remove the interference from the far user $\mathrm{D}_1$. Then, it decodes its own message. In this paper, we assume that $\mathrm{D}_2$ can perfectly remove interference. After that, the received signal at $\mathrm{D}_2$ from (9) can be rewritten as

$$y_{\mathrm{D}_2} = h_{\mathrm{RD}_2}\sqrt{a_2 P_{\mathrm{R}}}\, x_2 + z_2. \tag{10}$$

From equations (8)–(10), SINRs at $\mathrm{D}_1$ and $\mathrm{D}_2$ can be calculated as

$$\gamma_{\mathrm{D}_1}^{x_1} = \frac{\left|h_{\mathrm{RD}_1}\right|^2 a_1 P_{\mathrm{R}}}{\left|h_{\mathrm{RD}_1}\right|^2 a_2 P_{\mathrm{R}} + \sigma^2} = \frac{a_1\eta\alpha P\rho_2\rho_4}{a_2\eta\alpha P\rho_2\rho_4 + \sigma^2(1-\alpha)},$$

$$\gamma_{\mathrm{D}_2}^{\mathrm{SIC}_{x_1}} = \frac{\left|h_{\mathrm{RD}_2}\right|^2 a_1 P_{\mathrm{R}}}{\left|h_{\mathrm{RD}_2}\right|^2 a_2 P_{\mathrm{R}} + \sigma^2} = \frac{a_1\eta\alpha P\rho_2\rho_5}{a_2\eta\alpha P\rho_2\rho_5 + \sigma^2(1-\alpha)}, \tag{11}$$

$$\gamma_{\mathrm{D}_2}^{x_2} = \frac{\left|h_{\mathrm{RD}_2}\right|^2 a_2 P_{\mathrm{R}}}{\sigma^2} = \frac{a_2\eta\alpha P\rho_2\rho_5}{\sigma^2(1-\alpha)},$$

where $\rho_4 = |h_{\mathrm{RD}_1}|^2$ and $\rho_5 = |h_{\mathrm{RD}_2}|^2$ are the channel gains of the links R $\longrightarrow$ $\mathrm{D}_1$ and R $\longrightarrow$ $\mathrm{D}_2$, respectively.

It is also noted that, for DF relaying protocol, the end-to-end SINR is calculated as

$$\gamma_{\mathrm{e2e}} = \min\{\gamma_{\mathrm{R}}, \gamma_{\mathrm{D}}\}. \tag{12}$$

Therefore, the end-to-end SINRs at $\mathrm{D}_1$ and $\mathrm{D}_2$ can be written as follows:

$$\gamma_{\mathrm{D}_1} = \min\left\{\gamma_{\mathrm{R}}^{x_1}, \gamma_{\mathrm{D}_1}^{x_1}\right\}, \tag{13}$$

$$\gamma_{\mathrm{D}_2} = \min\left\{\gamma_{\mathrm{R}}^{x_1}, \gamma_{\mathrm{R}}^{x_2}, \gamma_{\mathrm{D}_2}^{\mathrm{SIC}_{x_1}}, \gamma_{\mathrm{D}_2}^{x_2}\right\}. \tag{14}$$

## 3. Performance Analysis

*3.1. Outage Probability Analysis.* In this section, the outage probability of the considered EH-FD-NOMA system is derived to evaluate the system performance. The system OP is the probability that makes the instantaneous SINR falling below a predefined threshold [29]. To derive OPs for this system, let $\mathscr{R}_1$ and $\mathscr{R}_2$ (bit/s/Hz) be the minimum required data rates for the users $\mathrm{D}_1$ and $\mathrm{D}_2$, respectively. By assuming the fairness of the users in this systems, we set $\mathscr{R}_1 = \mathscr{R}_2 = \mathscr{R}$. Then, OP at $\mathrm{D}_1$, denoted by $P_{\mathrm{out}}^{\mathrm{D}_1}$, can be calculated as

$$P_{\mathrm{out}}^{\mathrm{D}_1} = \Pr\left\{(1-\alpha)\log_2\left(1+\gamma_{\mathrm{D}_1}\right) < \mathscr{R}\right\} = \Pr\left\{\gamma_{\mathrm{D}_1} < 2^{\mathscr{R}/(1-\alpha)} - 1\right\}, \tag{15}$$

where $\gamma_{\mathrm{D}_1}$ is derived in (13). Let $x = 2^{\mathscr{R}/(1-\alpha)} - 1$ be the SINR threshold. Then, the expression (15) can be rewritten as

$$P_{\mathrm{out}}^{\mathrm{D}_1} = \Pr\left\{\gamma_{\mathrm{D}_1} < x\right\}. \tag{16}$$

At destination $\mathrm{D}_2$, the outage occurs when it does not decode successfully the signal $x_1$ or its own message $x_2$. Therefore, we have

$$P_{\text{out}}^{\text{D}_2} = \Pr\left\{\gamma_{\text{D}_2} < x\right\} = \Pr\left\{\min\left(\gamma_{\text{R}}^{x_1}, \gamma_{\text{R}}^{x_2}, \gamma_{\text{D}_2}^{\text{SIC}_{x_1}}, \gamma_{\text{D}_2}^{x_2}\right) < x\right\}$$
$$= \Pr\left\{\min\left[\min\left(\gamma_{\text{R}}^{x_1}, \gamma_{\text{R}}^{x_2}\right), \min\left(\gamma_{\text{D}_2}^{\text{SIC}_{x_1}}, \gamma_{\text{D}_2}^{x_2}\right)\right] < x\right\}. \tag{17}$$

**Theorem 1.** *The OPs at $D_1$ ($P_{out}^{D_1}$) and $D_2$ ($P_{out}^{D_2}$) of the cooperative EH-FD-NOMA system under the impact of RSI over Rayleigh fading channel are determined, respectively, as follows:*

$$P_{\text{out}}^{\text{D}_1} = \begin{cases} 1 - \sqrt{\dfrac{XYx^2}{(a_1 - a_2x)^2}} K_1\left(\sqrt{\dfrac{Xx}{a_1 - a_2x}}\right) K_1\left(\sqrt{\dfrac{Yx}{a_1 - a_2x}}\right), & x < \dfrac{a_1}{a_2}, \\ 1, & x \geq \dfrac{a_1}{a_2}, \end{cases} \tag{18}$$

$$P_{\text{out}}^{\text{D}_2} = \begin{cases} 1 - \sqrt{\dfrac{XZx^2}{a_2^2}} K_1\left(\sqrt{\dfrac{Xx}{a_2}}\right) K_1\left(\sqrt{\dfrac{Zx}{a_2}}\right), & x < \dfrac{a_1}{a_2} - 1, \\ 1 - \sqrt{\dfrac{XZx^2}{(a_1 - a_2x)^2}} K_1\left(\sqrt{\dfrac{Xx}{a_1 - a_2x}}\right) K_1\left(\sqrt{\dfrac{Zx}{a_1 - a_2x}}\right), & \dfrac{a_1}{a_2} - 1 \leq x < \dfrac{a_1}{a_2}, \\ 1, & x \geq \dfrac{a_1}{a_2}, \end{cases} \tag{19}$$

*where $X = (4(\gamma_{RSI} + \sigma^2)(1-\alpha))/(\Omega_1\Omega_3\eta\alpha P)$, $Y = (4\sigma^2(1-\alpha))/(\Omega_2\Omega_4\eta\alpha P)$, and $Z = (4\sigma^2(1-\alpha))/(\Omega_2\Omega_5\eta\alpha P)$. Here, $\Omega_i = \mathbb{E}\{\rho_i\}$ where $\Omega_i$ and $\rho_i$ denote the average and instantaneous channel gains of the Rayleigh fading channel, respectively ($i = 1, 2, \ldots, 5$); $\mathbb{E}$ denotes the expectation operator; and $K_1(\cdot)$ is the first-order modified Bessel function of the second kind [30].*

*Proof of Theorem 1.* To calculate $P_{\text{out}}^{\text{D}_1}$ and $P_{\text{out}}^{\text{D}_2}$, from equations (16) and (17), we apply the probability rule in [31] to get

$$P_{\text{out}}^{\text{D}_1} = \Pr\left\{\min\left(\gamma_{\text{R}}^{x_1}, \gamma_{\text{D}_1}^{x_1}\right) < x\right\} = \Pr\left\{\gamma_{\text{R}}^{x_1} < x\right\} + \Pr\left\{\gamma_{\text{D}_1}^{x_1} < x\right\}$$
$$- \Pr\left\{\gamma_{\text{R}}^{x_1} < x\right\}\Pr\left\{\gamma_{\text{D}_1}^{x_1} < x\right\}. \tag{20}$$

$$P_{\text{out}}^{\text{D}_2} = \Pr\left\{\min\left[\min\left(\gamma_{\text{R}}^{x_1}, \gamma_{\text{R}}^{x_2}\right), \min\left(\gamma_{\text{D}_2}^{\text{SIC}_{x_1}}, \gamma_{\text{D}_2}^{x_2}\right)\right] < x\right\}$$
$$= \Pr\left\{\min\left(\gamma_{\text{R}}^{x_1}, \gamma_{\text{R}}^{x_2}\right) < x\right\} + \Pr\left\{\min\left(\gamma_{\text{D}_2}^{\text{SIC}_{x_1}}, \gamma_{\text{D}_2}^{x_2}\right) < x\right\}$$
$$- \Pr\left\{\min\left(\gamma_{\text{R}}^{x_1}, \gamma_{\text{R}}^{x_2}\right) < x\right\}\Pr\left\{\min\left(\gamma_{\text{D}_2}^{\text{SIC}_{x_1}}, \gamma_{\text{D}_2}^{x_2}\right) < x\right\}. \tag{21}$$

On the contrary, the cumulative distribution functions (CDFs) $F_{\rho_i}(x)$ and probability distribution functions (PDFs) of the Rayleigh distribution $f_{\rho_i}(x)$ can be determined as follows:

$$F_{\rho_i}(x) = 1 - \exp\left(-\frac{x}{\Omega_i}\right), \quad x \geq 0, \tag{22}$$

$$f_{\rho_i}(x) = \frac{1}{\Omega_i}\exp\left(-\frac{x}{\Omega_i}\right), \quad x \geq 0. \tag{23}$$

By using equations (20)–(23) and doing some algebras, we can derive (18) and (19) in Theorem 1. For details of the proof, see in appendix A. □

*3.2. Ergodic Capacity Analysis.* The ergodic capacity of the FD relay system is calculated by

$$C = \mathbb{E}\{\log_2(1+\gamma)\} = \int_0^\infty \log_2(1+\gamma) f_\gamma(\gamma)\mathrm{d}\gamma, \tag{24}$$

where $\gamma$ is the end-to-end SINR of the considered system and $f_\gamma(\gamma)$ is the PDF of $\gamma$. To derive the closed-form expression of the ergodic capacity of the system, we rewrite (24) after some algebras as

$$C = \frac{1}{\ln 2}\int_0^\infty \frac{1 - F(x)}{1+x}\mathrm{d}x, \tag{25}$$

where $F(x)$ is the CDF of the end-to-end SINR of the considered system.

**Theorem 2.** *The ergodic capacities of both users $D_1$ and $D_2$ are, respectively, given by*

$$C_{D_1} = \frac{a_1\pi}{2Na_2\ln 2}\sum_{n=1}^{N}\sqrt{1-\phi_n^2}G_1(u), \tag{26}$$

$$C_{D_2} = \frac{\pi}{2N\ln 2}\left[\frac{a_1-a_2}{a_2}\sum_{n=1}^{N}\sqrt{1-\phi_n^2}G_{21}(v_1) + \sum_{n=1}^{N}\sqrt{1-\phi_n^2}G_{22}(v_2)\right], \tag{27}$$

*where $N$ is the complexity-accuracy trade-off parameter, $\phi_n = \cos((2n-1)\pi/2N)$, $u = (a_1/2a_2)(\phi_n+1)$, $v_1 = ((a_1-a_2)/2a_2)(\phi_n+1)$, and $v_2 = ((2a_1-a_2)/2a_2) + ((1/2)\phi_n)$.*

$$G_1(u) = \frac{1}{1+u}\sqrt{\frac{XYu^2}{(a_1-a_2u)^2}}\cdot K_1\left(\sqrt{\frac{Xu}{a_1-a_2u}}\right)K_1\left(\sqrt{\frac{Yu}{a_1-a_2u}}\right),$$

$$G_{21}(v_1) = \frac{1}{1+v_1}\sqrt{\frac{XZv_1^2}{a_2^2}}K_1\left(\sqrt{\frac{Xv_1}{a_2}}\right)K_1\left(\sqrt{\frac{Zv_1}{a_2}}\right),$$

$$G_{22}(v_2) = \frac{1}{1+v_2}\sqrt{\frac{XZv_2^2}{(a_1-a_2v_2)^2}}\cdot K_1\left(\sqrt{\frac{Xv_2}{a_1-a_2v_2}}\right)K_1\left(\sqrt{\frac{Zv_2}{a_1-a_2v_2}}\right). \tag{28}$$

*Proof of Theorem 2.* From (25), we calculate the ergodic capacities at $D_1$ ($C_{D_1}$) and $D_2$ ($C_{D_2}$) by replacing $F(x)$ in (25) by $P_{\text{out}}^{D_1}$ and $P_{\text{out}}^{D_2}$ in (18) and (19), respectively. Therefore, $C_{D_1}$ and $C_{D_2}$ are calculated as

$$C_{D_1} = \frac{1}{\ln 2}\int_0^\infty \frac{1-P_{\text{out}}^{D_1}(x)}{1+x}\mathrm{d}x, \tag{29}$$

$$C_{D_2} = \frac{1}{\ln 2}\int_0^\infty \frac{1-P_{\text{out}}^{D_2}(x)}{1+x}\mathrm{d}x. \tag{30}$$

By applying the integral formulas in [32], we obtain the ergodic capacities at $D_1$ and $D_2$ in (26) and (27) after some mathematical transforms. In appendix B, we provide the details of proof. □

## 4. Numerical Results

In this section, the EH-FD-NOMA system performance in terms of OP and ergodic capacity is plotted by using the expressions in Theorem 1 and Theorem 2. In addition, we also conduct the Monte-Carlo simulations on OP and ergodic capacity to demonstrate the correctness of theoretical formulas. The system performance is evaluated for different values of the average SNR, where SNR is the ratio between the transmit power of PB and the variance of AWGN, i.e., SNR = $P/\sigma^2$. In our simulations, we choose parameters for evaluating the system performance as follows: the power allocation coefficients are $a_1 = 0.65$ and $a_2 = 0.35$, the energy harvesting efficiency at each node is $\eta = 0.85$, the average channel gains $\Omega_1 = \Omega_2 = \Omega_3 = \Omega_5 = 1$, and $\Omega_4 = 0.7$. The simulation results were obtained by using $10^6$ channel realizations.

In Figure 3, we consider the OPs of both users $D_1$ and $D_2$ versus the average SNR. In this figure, we use the results of Theorem 1 to plot theoretical curves ((18) for $D_1$ and (19) for $D_2$) with $\alpha = 0.5$, $\mathscr{R} = 0.3$ bit/s/Hz, and SI cancellation capability $\widetilde{\Omega} = -30$ dB. It is obvious that the simulation curves exactly match with the theoretical ones. As can be seen from the figure, OPs of both users have the same performance and diversity order. They decrease when SNR increases. On the contrary, at high SNR regime (SNR > 35 dB), the OPs of both users decrease slowly. If we continuously increase SNR, the OPs will go to outage floor due to the RSI and NOMA coefficients. It is easy to see that, even if the RSI is very small and with high transmit power at PB, from (6) we have $\gamma_R^{x_1} \longrightarrow (a_1/a_2)$. If the RSI is larger, the outage floor will be reached sooner. Therefore, it is necessary to apply various SI cancellation techniques for the FD mode to avoid performance loss of the FD communication systems.

Figure 4 illustrates the throughput of the EH-FD-NOMA system versus average SNR with various data transmission rates $\mathscr{R} = 0.3; 0.5; 0.7$ bit/s/Hz. It is also noted that the system throughput is defined by $\mathscr{T}_{D_1} \triangleq \mathscr{R}(1-P_{\text{out}}^{D_1})$ and $\mathscr{T}_{D_2} \triangleq \mathscr{R}(1-P_{\text{out}}^{D_2})$. The other simulation parameters are the same as those in Figure 3. Figure 4 shows that at low SNR regime (i.e., SNR < 10 dB), with low data transmission rate, i.e., $\mathscr{R} = 0.3$, the throughput will reach the best value among three considered cases. When SNR increases, such as from 14 to 26 dB, the optimal throughput is obtained when $\mathscr{R} = 0.5$. In the case of SNR > 26 dB, the system throughput reaches the maximal value with $\mathscr{R} = 0.7$. Therefore, depending on the transmit power at PB, we can suitably choose the data transmission rate for the considered system to get the optimal throughput and improve the overall system performance.

Figure 5 shows the impact of EH time-switching ratio $\alpha$ on the OPs of the considered system with $\mathscr{R} = 0.3$ bit/s/Hz and $\widetilde{\Omega} = -30$ dB. As can be seen from the figure, there is an optimal value of $\alpha$ corresponding to a pretransmit power of PB. For example, with SNR = 20 dB, the optimal value is $\alpha \approx 0.6$. In the case of SNR = 30 dB, the value is $\alpha \approx 0.5$, and in the case of SNR = 40 dB, $\alpha \approx 0.3$. Consequently, based on the transmit power at PB, we can adjust the EH time-switching ratio in order to improve the system performance.

Figure 6 illustrates the ergodic capacity of both users under the impact of SI cancellation capability with $\widetilde{\Omega} = -30, -20$, and $-10$ dB. In this figure, the theoretical curves are plotted by using equations (26) and (27) in Theorem 2, while the marker symbols are plotted by Monte-Carlo simulations. It is obvious that the ergodic capacity increases when SNR increases, especially when

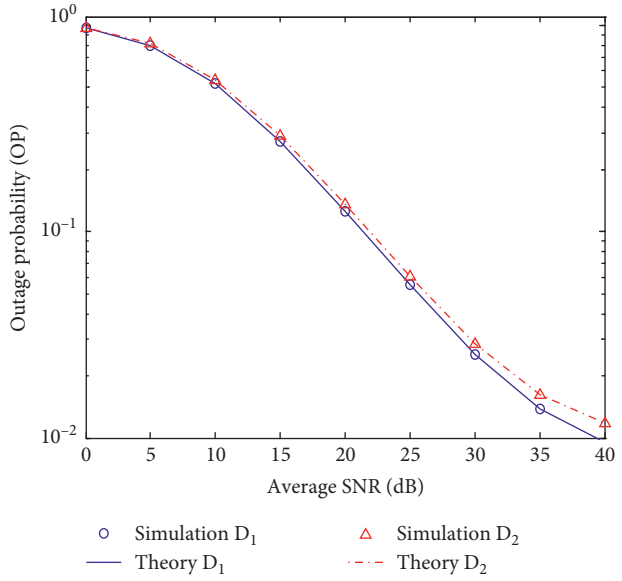


FIGURE 3: The OPs at $D_1$ and $D_2$ versus the average SNR when $\mathscr{R} = 0.3$ bit/s/Hz, $\widetilde{\Omega} = -30$ dB, and $\alpha = 0.5$.

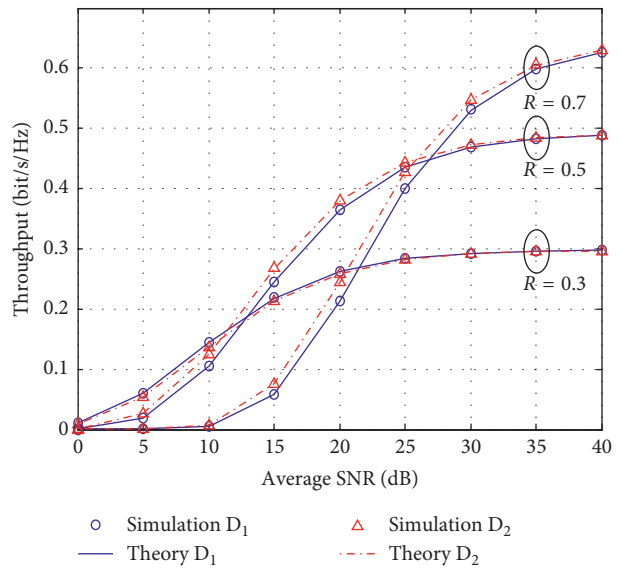


FIGURE 4: Throughput of the EH-FD-NOMA system with various data transmission rates $\mathscr{R} = 0.3; 0.5; 0.7$ bit/s/Hz.

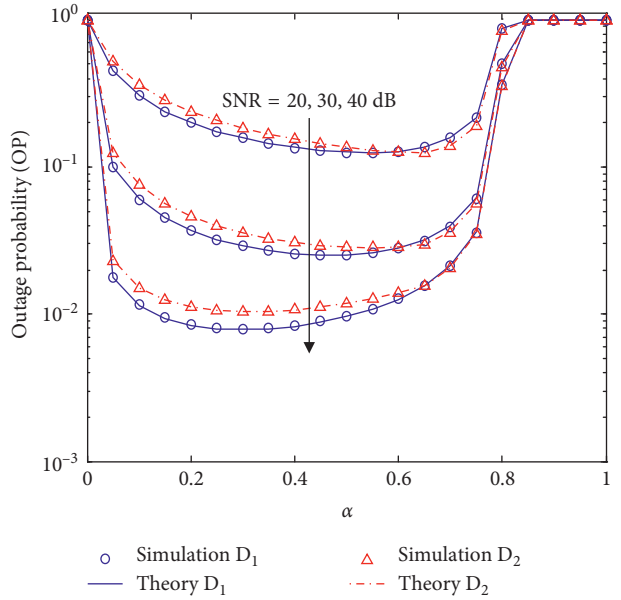


FIGURE 5: The impact of EH time duration on the OPs at both users with SNR = 20, 30, 40 dB, $\mathscr{R} = 0.3$ bit/s/Hz, and $\widetilde{\Omega} = -30$ dB.

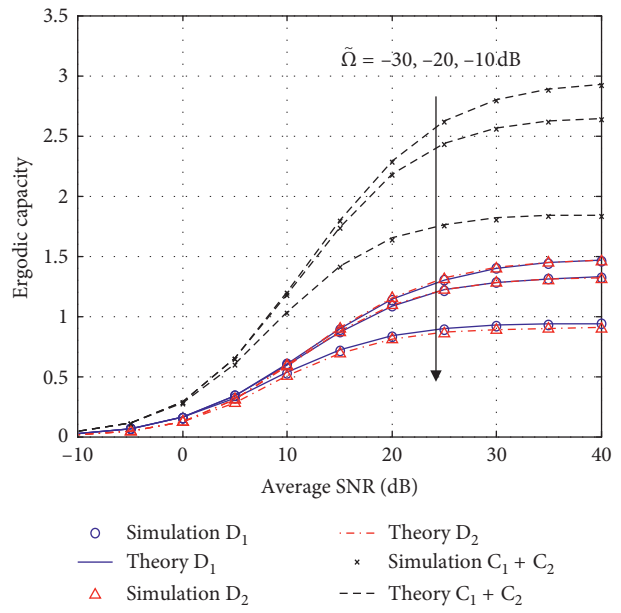


FIGURE 6: The ergodic capacities of both users under the impact of SI cancellation capability with $\alpha = 0.5$ and various levels of RSI.

RSI is small such as $\widetilde{\Omega} = -30$ dB. In the case of $\widetilde{\Omega} = -30$ dB, the ergodic capacity at both users increases about 0.6 bit/s/Hz comparing with the case of $\widetilde{\Omega} = -10$ dB. The gain for the system capacity is about 1.2 bit/s/Hz. Figure 6 shows the strong impact of RSI on the capacity of the considered system. Thus, to deploy this system in realistic scenarios, wireless researchers and designers need to design circuits and build algorithms in order to improve the SI cancellation.

Finally, Figure 7 plots the ergodic capacities of the EH-FD-NOMA system with various time durations of $\alpha$ in the case of $\widetilde{\Omega} = -30$ dB. This figure shows that the ergodic capacities of users $D_1$ and $D_2$ increase when $\alpha$ increases. For example, the ergodic capacity in the case of $\alpha = 0.7$ is the best capacity compared with the case of $\alpha = 0.3$ and $\alpha = 0.5$. However, at high SNR, such as SNR = 40 dB, the ergodic capacities of three considered cases are the same. The results in Figure 7 are compatible with those in Figure 5. By combining Figures 5 and 7, we can clearly see that when SNR < 30 dB, we choose $\alpha = 0.7$ to get the best performance and best capacity of the considered system.

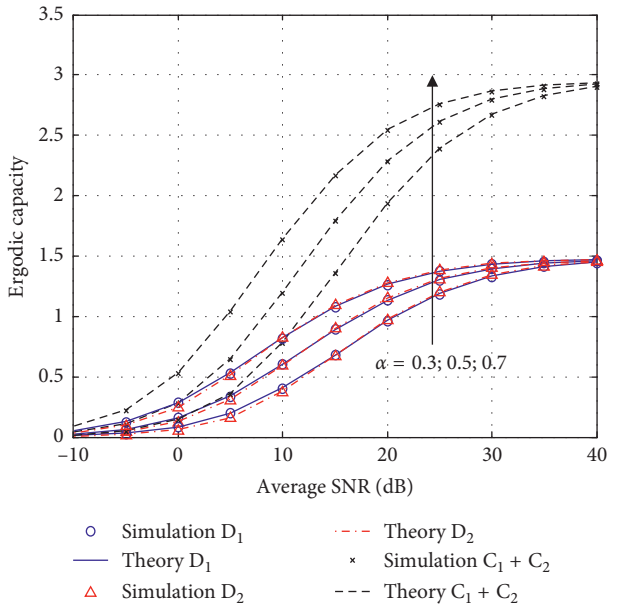


FIGURE 7: The impact of the EH time duration on the ergodic performance of the EH-FD-NOMA system versus the average SNR for different values of $\alpha$, $\alpha = 0.3; 0.5; 0.7$ and $\tilde{\Omega} = -30$ dB.

## 5. Conclusion

In this paper, we propose a novel combination of three advanced techniques, namely, EH, FD, and NOMA, in a so-called EH-FD-NOMA communication system, which can be applied for V2V communication networks. By mathematical analysis, we derive exact expressions of outage probability and ergodic capacity at both users under the impact of residual self-interference at the FD relay node. Our results show that the two users can obtain the same performance and capacity, i.e., the fairness is guaranteed. Depending on the transmit power at the power beacon, there is an optimal value for EH time-switching ratio to minimize the outage probability and maximize the capacity. Furthermore, the impact of data transmission rate, residual self-interference level, and time-switching factor $\alpha$ is also investigated. Numerical results demonstrate the importance of self-and-successive-interference cancellation on the performance of the considered system. Those results serve as important references for wireless researchers and designers in deployment of the EH-FD-NOMA system in practice.

## Appendix

## A. Proof of Theorem 1

In this appendix, we provide step-by-step procedure of how to derive the expressions of outage probability at both users of the proposed EH-FD-NOMA system over Rayleigh fading channels.

For $P_{\text{out}}^{D_1}$, from (20), we calculate $\Pr\{\gamma_R^{x_1} < x\}$ in (A.1) and $\Pr\{\gamma_{D_1}^{x_1} < x\}$ in (A.2) as follows:

$$\begin{aligned}\Pr\{\gamma_R^{x_1} < x\} &= \Pr\{\eta\alpha P(a_1 - a_2x)\rho_1\rho_3 < (\gamma_{RSI} + \sigma^2)(1-\alpha)x\} \\ &= \int_0^\infty F_{\rho_1}\left(\frac{(\gamma_{RSI} + \sigma^2)(1-\alpha)x}{\eta\alpha P(a_1 - a_2x)\rho_3}\right) f_{\rho_3}(\rho_3)d\rho_3 = \int_0^\infty \left[1 - \exp\left(-\frac{(\gamma_{RSI} + \sigma^2)(1-\alpha)x}{\Omega_1\eta\alpha P(a_1 - a_2x)\rho_3}\right)\right]\frac{1}{\Omega_3}\exp\left(-\frac{\rho_3}{\Omega_3}\right)d\rho_3 \\ &= 1 - \sqrt{\frac{4(\gamma_{RSI} + \sigma^2)(1-\alpha)x}{\Omega_1\Omega_3\eta\alpha P(a_1 - a_2x)}}K_1\left(\sqrt{\frac{4(\gamma_{RSI} + \sigma^2)(1-\alpha)x}{\Omega_1\Omega_3\eta\alpha P(a_1 - a_2x)}}\right) = 1 - \sqrt{\frac{Xx}{a_1 - a_2x}}K_1\left(\sqrt{\frac{Xx}{a_1 - a_2x}}\right).\end{aligned} \tag{A.1}$$

$$\begin{aligned}\Pr\{\gamma_{D_1}^{x_1} < x\} &= \Pr\{\eta\alpha P(a_1 - a_2x)\rho_2\rho_4 < \sigma^2(1-\alpha)x\} \\ &= \int_0^\infty F_{\rho_2}\left(\frac{\sigma^2(1-\alpha)x}{\eta\alpha P(a_1 - a_2x)\rho_4}\right) f_{\rho_4}(\rho_4)d\rho_4 = \int_0^\infty \left[1 - \exp\left(-\frac{\sigma^2(1-\alpha)x}{\Omega_2\eta\alpha P(a_1 - a_2x)\rho_4}\right)\right]\frac{1}{\Omega_4}\exp\left(-\frac{\rho_4}{\Omega_4}\right)d\rho_4 \\ &= 1 - \sqrt{\frac{4\sigma^2(1-\alpha)x}{\Omega_2\Omega_4\eta\alpha P(a_1 - a_2x)}}K_1\left(\sqrt{\frac{4\sigma^2(1-\alpha)x}{\Omega_2\Omega_4\eta\alpha P(a_1 - a_2x)}}\right) = 1 - \sqrt{\frac{Yx}{a_1 - a_2x}}K_1\left(\sqrt{\frac{Yx}{a_1 - a_2x}}\right).\end{aligned} \tag{A.2}$$

It is noted that, in the case of $a_1 - a_2x \le 0$, the probabilities in (A.1) and (A.2) always occur. Therefore, $\Pr\{\gamma_R^{x_1} < x\} = 1$ and $\Pr\{\gamma_{D_1}^{x_1} < x\} = 1$, which lead to $P_{\text{out}}^{D_1} = 1$. After doing some algebras and applying [30, 3.324.1], we derive $\Pr\{\gamma_R^{x_1} < x\}$ and $\Pr\{\gamma_{D_1}^{x_1} < x\}$ at the end of (A.1) and (A.2). By substituting (A.1) and (A.2) into (20), we obtain $P_{\text{out}}^{D_1}$ in (18) in Theorem 1.

For $P_{\text{out}}^{D_2}$, based on the equation (21), we can calculate $\Pr\{\min(\gamma_R^{x_1}, \gamma_R^{x_2}) < x\}$ as in (A.3) and $\Pr\{\min(\gamma_{D_2}^{\text{SIC}_{x_1}}, \gamma_{D_2}^{x_2}) < x\}$ as in (A.4):

$$\begin{aligned}\Pr\{\min(\gamma_R^{x_1},\gamma_R^{x_2})<x\} &= \Pr\left\{\min\left(\frac{a_1\eta\alpha P\rho_1\rho_3}{a_2\eta\alpha P\rho_1\rho_3+(\gamma_{RSI}+\sigma^2)(1-\alpha)},\frac{a_2\eta\alpha P\rho_1\rho_3}{(\gamma_{RSI}+\sigma^2)(1-\alpha)}\right)<x\right\}\\ &= \Pr\left\{\min\left(\eta\alpha P(a_1-a_2x)\rho_1\rho_3,\eta\alpha Pa_2\rho_1\rho_3\right)<\left(\gamma_{RSI}+\sigma^2\right)(1-\alpha)x\right\}\\ &= \begin{cases}\Pr\{\eta\alpha P(a_1-a_2x)\rho_1\rho_3<(\gamma_{RSI}+\sigma^2)(1-\alpha)x\}, & x\ge\dfrac{a_1}{a_2}-1\\ \Pr\{\eta\alpha Pa_2\rho_1\rho_3<(\gamma_{RSI}+\sigma^2)(1-\alpha)x\}, & x<\dfrac{a_1}{a_2}-1\end{cases}\\ &= \begin{cases}1-\sqrt{\dfrac{Xx}{a_1-a_2x}}K_1\left(\sqrt{\dfrac{Xx}{a_1-a_2x}}\right), & x\ge\dfrac{a_1}{a_2}-1\\ 1-\sqrt{\dfrac{Xx}{a_2}}K_1\left(\sqrt{\dfrac{Xx}{a_2}}\right), & x<\dfrac{a_1}{a_2}-1,\end{cases}\end{aligned} \tag{A.3}$$

$$\begin{aligned}\Pr\left\{\min\left(\gamma_{D_2}^{SIC_{x_1}},\gamma_{D_2}^{x_2}\right)<x\right\} &= \Pr\left\{\min\left(\frac{a_1\eta\alpha P\rho_2\rho_5}{a_2\eta\alpha P\rho_2\rho_5+\sigma^2(1-\alpha)},\frac{a_2\eta\alpha P\rho_2\rho_5}{\sigma^2(1-\alpha)}\right)<x\right\}\\ &= \Pr\left\{\min\left(\eta\alpha P(a_1-a_2x)\rho_2\rho_5,\eta\alpha Pa_2\rho_2\rho_5\right)<\sigma^2(1-\alpha)x\right\}\\ &= \begin{cases}\Pr\{\eta\alpha P(a_1-a_2x)\rho_2\rho_5<\sigma^2(1-\alpha)x\}, & x\ge\dfrac{a_1}{a_2}-1\\ \Pr\{\eta\alpha Pa_2\rho_2\rho_5<\sigma^2(1-\alpha)x\}, & x<\dfrac{a_1}{a_2}-1\end{cases}\\ &= \begin{cases}1-\sqrt{\dfrac{Zx}{a_1-a_2x}}K_1\left(\sqrt{\dfrac{Zx}{a_1-a_2x}}\right), & x\ge\dfrac{a_1}{a_2}-1\\ 1-\sqrt{\dfrac{Zx}{a_2}}K_1\left(\sqrt{\dfrac{Zx}{a_2}}\right), & x<\dfrac{a_1}{a_2}-1.\end{cases}\end{aligned} \tag{A.4}$$

It is also noted that when $a_1-a_2x\le 0$, we always have $P_{out}^{D_2}=1$. In the case of $a_1-a_2x\le a_2$, we have $x\ge(a_1/a_2)-1$, that means $\min(\eta\alpha P(a_1-a_2x)\rho_1\rho_3, \eta\alpha Pa_2\rho_1\rho_3)=\eta\alpha P(a_1-a_2x)\rho_1\rho_3$. Otherwise, we have $\min(\eta\alpha P(a_1-a_2x)\rho_1\rho_3,\eta\alpha Pa_2\rho_1\rho_3)=\eta\alpha Pa_2\rho_1\rho_3$. Therefore, we can transform the second line to the third line of (A.3) and (A.4). After doing some algebraic manipulations and using [30, 3.324.1], we obtain the final expressions of $\Pr\{\min(\gamma_R^{x_1},\gamma_R^{x_2})<x\}$ in the last line of (A.3) and $\Pr\left\{\min(\gamma_{D_2}^{SIC_{x_1}},\gamma_{D_2}^{x_2})<x\right\}$ in the last line of (A.4). After that, we can substitute (A.3) and (A.4) into (21) to achieve (19) as in Theorem 1.

The proof is complete.

## B. Proof of Theorem 2

This appendix is used to provide the detailed proof of Theorem 2. From (29) and (30), we have

$$C_{D_1}=\frac{1}{\ln 2}\int_0^{a_1/a_2}\frac{\sqrt{XYx^2/(a_1-a_2x)^2}K_1\left(\sqrt{Xx/(a_1-a_2x)}\right)K_1\left(\sqrt{Yx/(a_1-a_2x)}\right)}{1+x}dx, \tag{B.1}$$

$$\begin{aligned}C_{D_2} &= \frac{1}{\ln 2}\int_0^{a_1/a_2-1}\frac{\sqrt{(XZx^2/a_2^2)}K_1\left(\sqrt{(Xx/a_2)}\right)K_1\left(\sqrt{(Zx/a_2)}\right)}{1+x}dx\\ &\quad+\frac{1}{\ln 2}\int_{(a_1/a_2)-1}^{a_1/a_2}\frac{\sqrt{\left(XZx^2/(a_1-a_2x)^2\right)}K_1\left(\sqrt{(Xx/(a_1-a_2x))}\right)K_1\left(\sqrt{(Zx/(a_1-a_2x))}\right)}{1+x}dx.\end{aligned} \tag{B.2}$$

Due to the complexity of equations (B.1) and (B.2), it is difficult to derive the closed-form expressions for ergodic capacity at both users. In this case, we apply the Gaussian–Chebyshev quadrature method in [32] to obtain the ergodic capacity for both users.

The first and second terms in (B.2) are, respectively, calculated as

$$\frac{1}{\ln 2}\int_0^{(a_1/a_2)-1}\frac{\sqrt{(XZx^2/a_2^2)}K_1\left(\sqrt{(Xx/a_2)}\right)K_1\left(\sqrt{(Zx/a_2)}\right)}{1+x}\mathrm{d}x=\frac{\pi(a_1-a_2)}{2Na_2\ln 2}\sum_{n=1}^{N}\sqrt{1-\phi_n^2}G_{21}(v_1), \tag{B.3}$$

$$\frac{1}{\ln 2}\int_{(a_1/a_2)-1}^{a_1/a_2}\frac{\sqrt{\left(XZx^2/(a_1-a_2x)^2\right)}K_1\left(\sqrt{Xx/(a_1-a_2x)}\right)K_1\left(\sqrt{(Zx/(a_1-a_2x))}\right)}{1+x}\mathrm{d}x=\frac{\pi}{2N\ln 2}\sum_{n=1}^{N}\sqrt{1-\phi_n^2}G_{22}(v_2). \tag{B.4}$$

By substituting (B.3) and (B.4) into (B.2), we obtain the capacity of user $D_2$ as in (27). Similarly, the capacity of user $D_1$ is obtained as in (26).

The proof is complete.

## Data Availability

The simulation data used to support the findings of this study are included within the article.

## Conflicts of Interest

The authors declare that they have no conflicts of interest.

## Acknowledgments

This research is funded by the Vietnam National Foundation for Science and Technology Development (NAFOSTED) under grant number 102.04-2017.317.

## References

[1] S. Hong, J. Brand, J. Choi et al., "Applications of self-interference cancellation in 5G and beyond," *IEEE Communications Magazine*, vol. 52, no. 2, pp. 114–121, 2014.

[2] Q. C. Li, H. Niu, A. T. Papathanassiou, and G. Wu, "5G network capacity: key elements and technologies," *IEEE Vehicular Technology Magazine*, vol. 9, no. 1, pp. 71–78, 2014.

[3] B. C. Nguyen, T. M. Hoang, and L. T. Dung, "Performance analysis of vehicle-to-vehicle communication with full-duplex amplify-and-forward relay over double-Rayleigh fading channels," *Vehicular Communications*, vol. 19, Article ID 100166, 2019.

[4] O. Abbasi and A. Ebrahimi, "Cooperative noma with full-duplex amplify-and-forward relaying," *Transactions on Emerging Telecommunications Technologies*, vol. 29, no. 7, p. e3421, 2018.

[5] Y. Alsaba, C. Y. Leow, and S. K. Abdul Rahim, "Full-duplex cooperative non-orthogonal multiple access with beamforming and energy harvesting," *IEEE Access*, vol. 6, pp. 19726–19738, 2018.

[6] X. Yue, Y. Liu, S. Kang, A. Nallanathan, and Z. Ding, "Exploiting full/half-duplex user relaying in noma systems," *IEEE Transactions on Communications*, vol. 66, no. 2, pp. 560–575, 2017.

[7] Z. Zhang, Z. Ma, M. Xiao, Z. Ding, and P. Fan, "Full-duplex device-to-device-aided cooperative nonorthogonal multiple access," *IEEE Transactions on Vehicular Technology*, vol. 66, no. 5, pp. 4467–4471, 2017.

[8] G. Chen, P. Xiao, J. R. Kelly, B. Li, and R. Tafazolli, "Full-duplex wireless-powered relay in two way cooperative networks," *IEEE Access*, vol. 5, pp. 1548–1558, 2017.

[9] T. M. Hoang, V. Van Son, N. C. Dinh, and P. T. Hiep, "Optimizing duration of energy harvesting for downlink noma full-duplex over nakagami-m fading channel," *AEU-international Journal of Electronics and Communications*, vol. 95, pp. 199–206, 2018.

[10] B. C. Nguyen, T. M. Hoang, and P. T. Tran, "Performance analysis of full-duplex decode-and-forward relay system with energy harvesting over nakagami-m fading channels," *AEU-International Journal of Electronics and Communications*, vol. 98, pp. 114–122, 2019.

[11] T. N. Nguyen, P. T. Tran, and M. Vozňák, "Power splitting-based energy-harvesting protocol for wireless-powered communication networks with a bidirectional relay," *International Journal of Communication Systems*, vol. 31, no. 13, p. e3721, 2018.

[12] S. Mondal, S. Dhar Roy, and S. Kundu, "Primary behaviour-based energy harvesting multihop cognitive radio network," *IET Communications*, vol. 11, no. 16, pp. 2466–2475, 2017.

[13] M. R. Camana, P. V. Tuan, and I. Koo, "Optimised power allocation for a power beacon-assisted swipt system with a power-splitting receiver," *International Journal of Electronics*, vol. 106, no. 3, pp. 415–439, 2019.

[14] N. P. Le, "Outage probability analysis in power-beacon assisted energy harvesting cognitive relay wireless networks," *Wireless Communications and Mobile Computing*, vol. 2017, Article ID 2019404, 15 pages, 2017.

[15] S.-L. Wang and T.-M. Wu, "Stochastic geometric performance analyses for the cooperative noma with the full-duplex energy harvesting relaying," *IEEE Transactions on Vehicular Technology*, vol. 68, no. 5, pp. 4894–4905, 2019.

[16] C. Guo, L. Zhao, C. Feng, Z. Ding, and H.-H. Chen, "Energy harvesting enabled noma systems with full-duplex relaying," *IEEE Transactions on Vehicular Technology*, vol. 68, no. 7, pp. 7179–7183, 2019.

[17] X. Zhang and F. Wang, "Resource allocation for wireless power transmission over full-duplex ofdma/noma mobile wireless networks," *IEEE Journal on Selected Areas in Communications*, vol. 37, no. 2, pp. 327–344, 2019.

[18] A. H. Gazestani, S. A. Ghorashi, B. Mousavinasab, and M. Shikh-Bahaei, "A survey on implementation and applications of full duplex wireless communications," *Physical Communication*, vol. 34, pp. 121–134, 2019.

[19] X. Lu, P. Wang, D. Niyato, D. I. Kim, and Z. Han, "Wireless networks with rf energy harvesting: a contemporary survey," *IEEE Communications Surveys and Tutorials*, vol. 17, no. 2, pp. 757–789, 2015.

[20] C. Zhong, H. A. Suraweera, G. Zheng, I. Krikidis, and Z. Zhang, "Wireless information and power transfer with full duplex relaying," *IEEE Transactions on Communications*, vol. 62, no. 10, pp. 3447–3461, 2014.

[21] X. Zhou, R. Zhang, and C. K. Ho, "Wireless information and power transfer: architecture design and rate-energy tradeoff," *IEEE Transactions on Communications*, vol. 61, no. 11, pp. 4754–4767, 2013.

[22] B. C. Nguyen, X. N. Tran, and D. T. Tran, "Performance analysis of in-band full-duplex amplify-and-forward relay system with direct link," in *Proceedings of the 2018 2nd International Conference on Recent Advances in Signal Processing, Telecommunications & Computing (SigTelCom)*, pp. 192–197, IEEE, Ho Chi Minh, Vietnam, January 2018.

[23] A. Sabharwal, P. Schniter, D. Guo, D. W. Bliss, S. Rangarajan, and R. Wichman, "In-band full-duplex wireless: challenges and opportunities," *IEEE Journal on Selected Areas in Communications*, vol. 32, no. 9, pp. 1637–1652, 2014.

[24] K. Yang, H. Cui, L. Song, and Y. Li, "Efficient full-duplex relaying with joint antenna-relay selection and self-interference suppression," *IEEE Transactions on Wireless Communications*, vol. 14, no. 7, pp. 3991–4005, 2015.

[25] X. Li, C. Tepedelenlioglu, and H. Senol, "Channel estimation for residual self-interference in full duplex amplify-and-forward two-way relays," *IEEE Transactions on Wireless Communications*, vol. 16, no. 8, pp. 4970–4983, 2017.

[26] B. C. Nguyen and X. N. Tran, "Performance analysis of full-duplex amplify-and-forward relay system with hardware impairments and imperfect self-interference cancellation," *Wireless Communications and Mobile Computing*, vol. 2019, Article ID 4946298, 10 pages, 2019.

[27] X.-X. Nguyen, D.-T. Do, T. M. Hoang et al., "System performance of cooperative NOMA with full-duplex relay over nakagami-m fading channels," *Mobile Information Systems*, vol. 2019, pp. 1–12, 2019.

[28] X. N. Tran, B. C. Nguyen, and D. T. Tran, "Outage probability of two-way full-duplex relay system with hardware impairments," in *Proceedings of the 2019 3rd International Conference on Recent Advances in Signal Processing, Telecommunications & Computing (SigTelCom)*, pp. 135–139, IEEE, HaNoi, Vietnam, March 2019.

[29] A. Goldsmith, *Wireless Communications*, Cambridge University Press, Cambridge, UK, 2005.

[30] A. Jeffrey and D. Zwillinger, *Table of Integrals, Series, and Products*, Academic Press, Cambridge, MA, USA, 2007.

[31] A. Leon-Garcia and A. Leon-Garcia, *Probability, Statistics, and Random Processes for Electrical Engineering*, Pearson/Prentice Hall, Upper Saddle River, NJ, USA, 3rd edition, 2008.

[32] M. Abramowitz and I. A. Stegun, *Handbook of Mathematical Functions with Formulas, Graphs, and Mathematical Tables*, Vol. 9, Dover, New York, NY, USA, 1972.